Fractional Fokker-Planck dynamics: Numerical algorithm and simulations

E. Heinsalu,[1,2] M. Patriarca,[1] I. Goychuk,[1] G. Schmid,[1] and P. Hänggi[1]
[1]*Institut für Physik, Universität Augsburg, Universitätsstrasse 1, D-86135 Augsburg, Germany*
[2]*Institute of Theoretical Physics, Tartu University, Tähe 4, 51010 Tartu, Estonia*
(Received 27 February 2006; published 25 April 2006)

Anomalous transport in a tilted periodic potential is investigated numerically within the framework of the fractional Fokker-Planck dynamics via the underlying continuous-time random walk. An efficient numerical algorithm is developed which is applicable for an arbitrary potential. This algorithm is then applied to investigate the fractional current and the corresponding nonlinear mobility in different washboard potentials. Normal and fractional diffusion are compared through their time evolution of the probability density in state space. Moreover, we discuss the stationary probability density of the fractional current values.

DOI: 10.1103/PhysRevE.73.046133 PACS number(s): 02.50.Ey, 05.40.−a, 02.70.−c

I. INTRODUCTION

Thermal diffusion of Brownian particles under the action of a periodic force continues to present an active field of research over recent years, being relevant for various applications in condensed matter physics, chemical physics, nanotechnology, and molecular biology [1–6].

The stochastic motion of Brownian particles in a potential

$$U(x) = V(x) - Fx, \tag{1}$$

where $V(x)=V(x+L)$ is the periodic substrate potential with period L and F is the constant bias, is qualitatively well known [6,7]: Particles, subject to friction and noise, will diffuse and drift in the direction of the applied bias. In the overdamped regime and in the absence of noise, the particles perform a creeping motion. If the tilting force F is large enough, so that the total potential $U(x)$ has no minima, the particles move down the corrugated plane. If minima do exist, the particles arrive there and stop. In the presence of noise, the particles do not stay permanently in the minima but will undergo noise-activated escape events. The particles thus perform a hopping process from one well to the neighboring ones.

It is well known that among many other applications [6,7], the model of a Brownian particle in a periodic potential can be used to describe Brownian motors and molecular motors [8–11], such as kinesins, dyneins, and myosins. However, many other systems, such as RNA polymerases, exonuclease and DNA polymerases, helicases, the motion of ribosomes along mRNA, and the translocation of RNA or DNA through a pore, are advantageously described as particles moving along a disordered substrate. Depending on the statistical properties of the potential, the long-time limit of the process can be quite different from that in a washboard potential [12]. It has been shown that the heterogeneity of the substrate potential may lead to anomalous dynamics [13–16]. In particular, over a range of forces around the stall force subdiffusion is observed [12]; i.e., the displacement grows as $\langle \delta r^2(t) \rangle \sim t^\alpha$, with $0<\alpha<1$.

Given the importance of the subdiffusion and motion in periodic potentials in various applications [9,17,18] and considering the biological systems mentioned above, we address the physics of the effect of the combined action of a biased periodic force and a random substrate. Within our approach we model the subdiffusive dynamics in terms of a suitable residence time probability density with a long tail [14,15,19] rather than through a random potential [13,15,20].

The Fokker-Planck equation describing the overdamped Brownian motion in the potential $U(x)$ can be generalized to anomalous transport. The corresponding result is known as the *fractional Fokker-Planck equation* [18,21,22], being the central equation of fractional dynamics,

$$\frac{\partial}{\partial t}P(x,t) = {}_0\hat{D}_t^{1-\alpha}\left[\frac{\partial}{\partial x}\frac{U'(x)}{\eta_\alpha} + \kappa_\alpha \frac{\partial^2}{\partial x^2}\right]P(x,t). \tag{2}$$

In our notation $P(x,t)$ is the probability density, a prime stands for the derivative with respect to the space coordinate, and κ_α denotes the anomalous diffusion coefficient with physical dimension $[\mathrm{m}^2\,\mathrm{s}^{-\alpha}]$. The quantity η_α denotes the generalized friction coefficient possessing the dimension $[\mathrm{kg}\,\mathrm{s}^{\alpha-2}]$; it is related to κ_α through $\eta_\alpha\kappa_\alpha = k_B T$, thus constituting a generalized Einstein relation.

The notation ${}_0\hat{D}_t^{1-\alpha}$ on the right-hand side of Eq. (2) stands for the integro-differential operator of the Riemann-Liouville fractional derivative, defined as follows [18,23,24]:

$${}_0\hat{D}_t^{1-\alpha}P(x,t) = \frac{1}{\Gamma(\alpha)}\frac{\partial}{\partial t}\int_0^t dt' \frac{P(x,t')}{(t-t')^{1-\alpha}}, \tag{3}$$

for $0<\alpha<1$. The Riemann-Liouville operator (3) introduces a convolution integral with a slowly decaying power-law kernel, which is typical for memory effects in complex systems. Equation (2) describes subdiffusive processes for $0<\alpha<1$ and reduces to the ordinary Fokker-Planck equation when $\alpha=1$.

The fractional Fokker-Planck equation was originally introduced with the Riemann-Liouville fractional derivative on its right-hand side [18,23]. However, it can sometimes be more convenient to switch to an equivalent representation that involves the Caputo fractional derivative. This formulation can provide genuine technical advantages. The fractional Fokker-Planck equation can then be rewritten as

$$D_*^\alpha P(x,t) = \left[\frac{\partial}{\partial x} \frac{U'(x)}{\eta_\alpha} + \kappa_\alpha \frac{\partial^2}{\partial x^2} \right] P(x,t), \tag{4}$$

with the Caputo fractional derivative D_*^α on its left-hand side [24]—i.e.,

$$D_*^\alpha P(x,t) = \frac{1}{\Gamma(1-\alpha)} \int_0^t dt' \frac{1}{(t-t')^\alpha} \frac{\partial}{\partial t'} P(x,t'). \tag{5}$$

In the present work we investigate the anomalous transport described by the fractional Fokker-Planck equations (2) and (4) through numerical simulation of the corresponding continuous-time random walk (CTRW). In Sec. II we develop the algorithm for the numerical simulations. In Sec. III we study the fractional current and the mobility for various types of tilted periodic potentials and in Sec. IV the time evolution of the probability density in space as well as the density of the current values. In doing so we emphasize similarities and analogies between anomalous and normal diffusion. The implications of the differences are discussed in the Conclusions.

II. NUMERICAL SIMULATION OF THE FRACTIONAL FOKKER-PLANCK EQUATION THROUGH THE UNDERLYING CONTINUOUS-TIME RANDOM WALK

The fractional Fokker-Planck equation represents the continuous limit of a CTRW with the Mittag-Leffler residence time density [25]

$$\psi_i(\tau) = -\frac{d}{d\tau} E_\alpha(-(\nu_i \tau)^\alpha); \tag{6}$$

$E_\alpha(-(\nu_i\tau)^\alpha)$ is the Mittag-Leffler function,

$$E_\alpha(-(\nu_i\tau)^\alpha) = \sum_{n=0}^{\infty} \frac{[-(\nu_i\tau)^\alpha]^n}{\Gamma(n\alpha+1)}, \tag{7}$$

and the quantity ν_i^{-1} denotes the time-scaling parameter at site i.

The numerical algorithm of the CTRW can be readily implemented for motion in an arbitrary force field, as we will demonstrate below.

A. Numerical algorithm for the continuous-time random walk

To study the CTRW in an one-dimensional potential $U(x)$, we consider an ensemble of N particles moving on a lattice $\{x_i = i\Delta x\}$, with a lattice period Δx; $i = 0, \pm 1, \pm 2, \ldots$. We emphasize that the numerical algorithm that we provide is valid for an arbitrary potential—i.e., not only for the potential (1). The state of the nth particle is defined through its current position $x^{(n)}$ and the time $t^{(n)}$ at which it will perform the next jump to a nearest-neighbor site.

The nth particle of the ensemble starts from the initial position $x^{(n)}(t_0) = x_0^{(n)}$. After a residence time τ extracted from the probability density $\psi_i(\tau)$, the particle jumps from site i to site $i+1$ or $i-1$ with probability q_i^+ or q_i^-, respectively, obeying the normalization condition $q_i^+ + q_i^- = 1$. Correspondingly, the space coordinate and the time are updated, $x^{(n)} \to x^{(n)} \pm \Delta x$ and $t^{(n)} \to t^{(n)} + \tau$. Reiterating this procedure, the full random trajectory of the random walker can be computed (see Fig. 1).

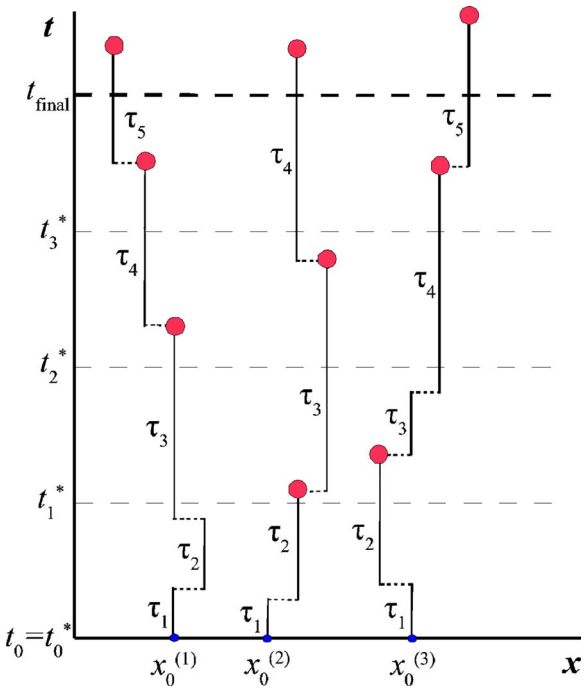

FIG. 1. (Color online) Sketch of the numerical algorithm: after a random waiting time τ the particle jumps from the current position $x^{(n)}$ to the position $x^{(n)}+\Delta x$ or $x^{(n)}-\Delta x$. The process is reiterated until $t^{(n)} \geqslant t_{\text{final}}$. The numerical measurements are performed after constant time intervals at times t_m^*. The solid circles represent the events that are used for the computation of the physical quantities (see text for an explanation).

In order to perform the numerical simulation, one needs to evaluate the quantities $q_i^\pm$ and ν_i. In terms of the fractional transition rates f_i and g_i, they can be expressed in the following way:

$$q_i^+ = f_i/(f_i+g_i), \quad q_i^- = g_i/(f_i+g_i), \tag{8}$$

$$\nu_i = (f_i+g_i)^{1/\alpha}, \tag{9}$$

where we have chosen

$$f_i = (\kappa_\alpha/\Delta x^2)\exp[-\beta(U_{i+1}-U_i)/2], \tag{10a}$$

$$g_i = (\kappa_\alpha/\Delta x^2)\exp[-\beta(U_{i-1}-U_i)/2]. \tag{10b}$$

Here $\beta = 1/k_B T$ is the inverse temperature and $U_i \equiv U(i\Delta x)$. An appropriate discretization step Δx has to satisfy the condition $|\beta(U_{i\pm1}-U_i)| \ll 1$ [26]. Furthermore, the condition $U''(x)\Delta x \ll 2U'(x)$ must be fulfilled, in order to ensure the smoothness of the potential. In the limit $\Delta x \to 0$ this so-constructed, limiting CTRW is described by the fractional Fokker-Planck equation (2) or, equivalently, through Eq. (4) [25].

In the case of a confining potential it is sufficient to compute the splitting probabilities $q_i^\pm$ and the time scale parameters ν_i only once over a finite x region at the beginning of

the simulation. In the case of a periodic or washboard potential, the quantities $q_i^{\pm}$ and ν_i can be computed only for the first period. In the latter case, while the total potential $U(x)$ is not periodic, the potential differences appearing in the fractional rates (10) can be rewritten as

$$U(x_i \pm \Delta x) - U(x_i) = V(x_i \pm \Delta x) - V(x_i) \mp F\Delta x$$

and are therefore periodic functions of x_i.

To perform the numerical measurements and compute the average $\langle Y(t)\rangle$ of a quantity $Y(t)=Y(x(t))$, we introduce a time lattice $\{t_m^*=m\Delta t^*\}$, where $m=0,1,\ldots,M$, and Δt^* is a constant time interval between two consecutive measurements. For the computation of the average $\langle Y(t)\rangle$, there are at least two different strategies, which we discuss here. Both methods can be illustrated through Fig. 1.

The first possibility is as follows: Each trajectory $x^{(n)}(t)$ is separately evolved with time, until the final time t_{final} is reached, $t^{(n)} \geqslant t_{\text{final}}$. As this nth trajectory reaches a measurement time t_m^* (represented with dashed lines in Fig. 1)—i.e., $t^{(n)} \geqslant t_m^*$—the quantity $Y_m^{(n)}=Y(x^{(n)}(t_m^*))$ will be computed using the coordinates corresponding to the events marked with solid circles in Fig. 1. The value $Y_m^{(n)}$ will be saved in a storage variable $Y_{\text{sum}}(t_m^*)=\Sigma_n Y_m^{(n)}$. After evolving all the N trajectories, the average is finally computed by normalization, $\langle Y(t_m^*)\rangle = Y_{\text{sum}}(t_m^*)/N$.

The second possibility is to evolve the whole ensemble until the times of all the trajectories $t^{(n)}$ (at which the particles will perform the next jump) exceed the fixed chosen measurement time t_m^*. We mark these events in Fig. 1 with solid circles. Then, all the corresponding positions $x^{(n)}$ and times $t^{(n)}$ will be saved and the average $\langle Y\rangle$ at the fixed time t_m^* will be computed. The procedure is reiterated to evolve the system until the final time t_{final}.

Which of the two methods is to be preferred depends on the problem studied and the available computational resources. We use the method in which the whole ensemble is evolved in time, since it allows one to save the system configuration (and therefore to stop and also restart the time evolution) and compute the average quantities after each measurement time t_m^*. Furthermore, evolving the whole system together allows one to simulate a set of N particles interacting with each other. This method also allows for single-trajectory averages.

B. Mittag-Leffler vs Pareto

According to the Tauberian theorems [27], for every $0<\alpha<1$ the long-time behavior of the system is determined solely by the tail of the residence time distribution [28]. Therefore, any other distribution with the same asymptotic form $S_\alpha(\nu_i\tau)\sim 1/\Gamma(1-\alpha)(\nu_i\tau)^\alpha$ could be used in place of the Mittag-Leffler distribution (7). In fact, also the conditions $S_\alpha(0)=1$ and $S_\alpha(x\to\infty)=0$ must be satisfied, and the function $S_\alpha(\nu_i\tau)$ has to decrease monotonically with τ.

The Mittag-Leffler function $E_\alpha(-\xi)$, defined by Eq. (7), can be numerically computed at $\xi<\xi_0$ through the sum

$$E_\alpha(-\xi) \approx \sum_{h=0}^{H} \frac{(-\xi)^h}{\Gamma(1+\alpha h)}, \tag{11}$$

while at values of $\xi>\xi_0$ its asymptotic expansion can be used,

$$E_\alpha(-\xi) \approx -\sum_{k=1}^{K} \frac{(\xi)^{-k}}{\Gamma(1-\alpha k)}, \tag{12}$$

with suitable values of H, K, and ξ_0.

A suitable choice for an approximate description is a Pareto probability density, defined by

$$\psi_i(\tau) = -\frac{d}{d\tau} P_\alpha(\nu_i\tau), \tag{13}$$

with the survival probability

$$P_\alpha(\nu_i\tau) = \frac{1}{[1+\Gamma(1-\alpha)^{1/\alpha}\nu_i\tau]^\alpha}. \tag{14}$$

In the simulations of the CTRW we have usually employed the Pareto distribution $y=P_\alpha(\nu_i\tau)$. It is convenient numerically because it can be readily inverted to provide a random residence time τ [29],

$$\tau = \nu_i^{-1}\frac{y^{-1/\alpha}-1}{\Gamma(1-\alpha)^{1/\alpha}}; \tag{15}$$

y is a uniform random number in $(0,1)$. Instead, the Mittag-Leffler distribution requires a specific algorithm to be inverted; e.g., we have used a look-up table with the values computed from Eqs. (11) and (12).

We have numerically verified the equivalence of the Mittag-Leffler and Pareto distributions in the computation of the asymptotic quantities. However, the difference in the behavior of the Mittag-Leffler and Pareto residence time distributions in the limit $\alpha\to 1$ has to be noticed: Namely, for $\alpha=1$ the Mittag-Leffler distribution transforms into the exponential function $E_1(-\nu_i\tau)\equiv\exp(-\nu_i\tau)$, while the Pareto distribution remains of a power-law type, leading to normal and anomalous diffusion, respectively. For this reason, when studying numerically fractional diffusion with $\alpha\to 1$ the Mittag-Leffler probability distribution should be used preferably.

As the Tauberian theorems ensure the equivalence of the Mittag-Leffler and Pareto distributions only in the asymptotic limit $t\to\infty$, it is to be expected that at finite times t the two choices for the probability densities provide different results. The difference increases as the parameter α approaches the value $\alpha=1$. This situation is illustrated through the example in Fig. 2.

C. Summary of the algorithm

Here we provide the core scheme of the time evolution algorithm used in the simulations and described above in Secs. II A and II B. The core of the program is the following one.

For every measurement time $t_m=m\Delta t^*$, where $m=1,\ldots,M$, the loop over trajectories is performed.

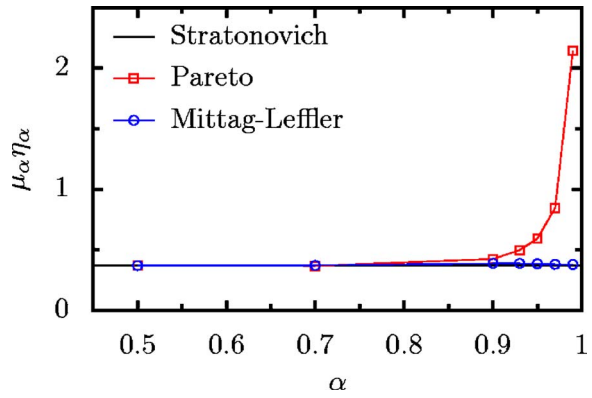

FIG. 2. (Color online) Rescaled mobility $\mu_\alpha(F)\eta_\alpha$ for $F/F_{\rm cr}=1$, as a function of α. After the same rescaled simulation time $t \approx 200$ (see Sec. III for the definition of the rescaled units), the distance from the asymptotic limit predicted by the Stratonovich formula (solid line) of the mobility values corresponding to the Pareto residence time density (squares) increases significantly for $\alpha > 0.9$, with respect to those of the Mittag-Leffler residence time density (circles).

(A) For every trajectory n, where $n=1,\ldots,N$, the following procedure is performed.

(i) While the next jumping time is smaller than the next measurement time, $t^{(n)} < m\Delta t^*$, the following steps are reiterated.

(a) From Eq. (9) the time scale parameter ν_i at the current position i is computed. A random waiting time τ is extracted from the residence time distribution (see Sec. II B), and the next jumping time is computed, $t^{(n)} \to t^{(n)} + \tau$.

(b) From Eqs. (8) the probabilities $q_i^{\pm}$ to perform the jump from site i to site $i \pm 1$ are computed. A uniform random number between 0 and 1 is extracted to determine whether the particle jumps to the right or left and the new position of the particle is then computed, $x^{(n)} \to x^{(n)} \pm \Delta x$.

(ii) The coordinate $x^{(n)}$ and the next jumping time $t^{(n)}$ are stored.

(B) Statistical averages at time $t_m = m\Delta t^*$ are computed using the stored coordinates $\{x^{(n)}\}$.

III. FRACTIONAL CURRENT AND GENERALIZED NONLINEAR MOBILITY IN WASHBOARD POTENTIALS

Starting out with the fractional Fokker-Planck equation in the form (4) one can derive the expression for the mean particle position in a one dimensional tilted periodic potential (1) [25], reading

$$\langle x(t)\rangle = \langle x(0)\rangle + \frac{v_\alpha(F)}{\Gamma(\alpha+1)} t^\alpha, \tag{16}$$

where the stationary fractional current is given by

$$v_\alpha(F) = \frac{\kappa_\alpha L[1-\exp(-\beta F L)]}{\int_0^L dx \int_x^{x+L} dy \exp\{-\beta[U(x)-U(y)]\}}. \tag{17}$$

This formula represents the anomalous counterpart of the current known for normal diffusion and reduces to the Stratonovich formula for $\alpha=1$ [6,30]. For completeness and for the reader's convenience a simple derivation of Eq. (17) is provided in the Appendix.

Numerically, the fractional current is computed in the following manner:

$$v_\alpha(F) = \Gamma(\alpha+1) \lim_{t\to\infty} \frac{\langle x(t)\rangle - \langle x(0)\rangle}{t^\alpha}. \tag{18}$$

The generalized nonlinear mobility is defined as

$$\mu_\alpha(F) = v_\alpha(F)/F, \tag{19}$$

where $F \neq 0$.

We test the validity of the generalized Stratonovich formula (17) obtained theoretically through the simulation of the fractional CTRW in different periodic potentials. We start out with (i) the symmetric cosine potential

$$V_1(x) = \cos(2\pi x/L). \tag{20}$$

As another type (ii) we consider the symmetric double-hump periodic potential

$$V_2(x) = [\cos(2\pi x/L) + \cos(4\pi x/L)]/2. \tag{21}$$

In order to explore the role of symmetries of the substrate potential we also consider (iii) the asymmetric (i.e., no reflection symmetry holds), ratchetlike periodic potential, reading

$$V_3(x) = [3\sin(2\pi x/L) + \sin(4\pi x/L)]/5. \tag{22}$$

The potentials in Eqs. (20)–(22), as well as the thermal energy k_BT, are measured in the same energy unit. For the sake of simplicity, the same symbol T is used in the following to represent the rescaled thermal energy.

In the numerical simulations we have used the Pareto probability density (13) for $0 < \alpha \leqslant 0.8$ and the Mittag-Leffler density (6) for $0.8 < \alpha < 1$ (see the discussion in Sec. II B). For $\alpha=1$ corresponding to a normal Brownian process we have employed the exponential residence time probability density

$$\psi_i(\tau) = -\frac{d}{d\tau}\exp(-\nu_i\tau). \tag{23}$$

As a space step we used $\Delta x = 0.001$, measured in units of the space period L. The energy is measured in units of the potential amplitude A, and the time unit is set as $\tau_0 = (\eta_\alpha L^2/A)^{1/\alpha}$. For the ensemble average we have employed 10^4 trajectories, each one starting from the same initial condition $x(t_0)=x_0$. The force is measured in units of the critical tilt $F_{\rm cr}$, which corresponds to the disappearance of potential extrema. In the case of the asymmetric ratchet potential the positive critical tilt is used.

We present in Figs. 3–5 the numerical results for the scaled fractional current $v_\alpha(F)/(F_{\rm cr}/\eta_\alpha)$ and the corresponding scaled nonlinear mobility—i.e., $\mu_\alpha(F)\eta_\alpha$, with $v_\alpha(F)$ and $\mu_\alpha(F)$ defined through Eqs. (18) and (19). The subcurrent is measured in units of $F_{\rm cr}/\eta_\alpha$—i.e., the subcurrent of a particle under the action of a constant bias $F=F_{\rm cr}$—the mobility is in units of the free mobility η_α^{-1}. Without loss of generality we have chosen $F>0$ for the symmetric substrate potentials (20)

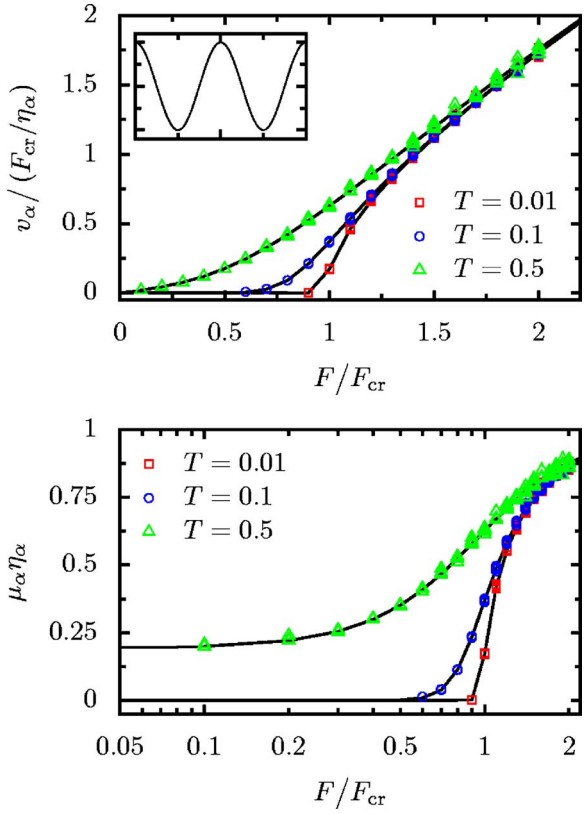

FIG. 3. (Color online). Dimensionless subcurrent $v_\alpha(F)/(F_{cr}/\eta_\alpha)$ and nonlinear mobility $\mu_\alpha(F)\eta_\alpha$ for the case of the cosine substrate potential, cf. Eq. (20) (depicted in the inset) vs F/F_{cr}. Numerical values corresponding to different temperatures T and fractional exponents $\alpha \in [0.1,1]$ (symbols) fit the analytic predictions from Eq. (17) (solid lines).

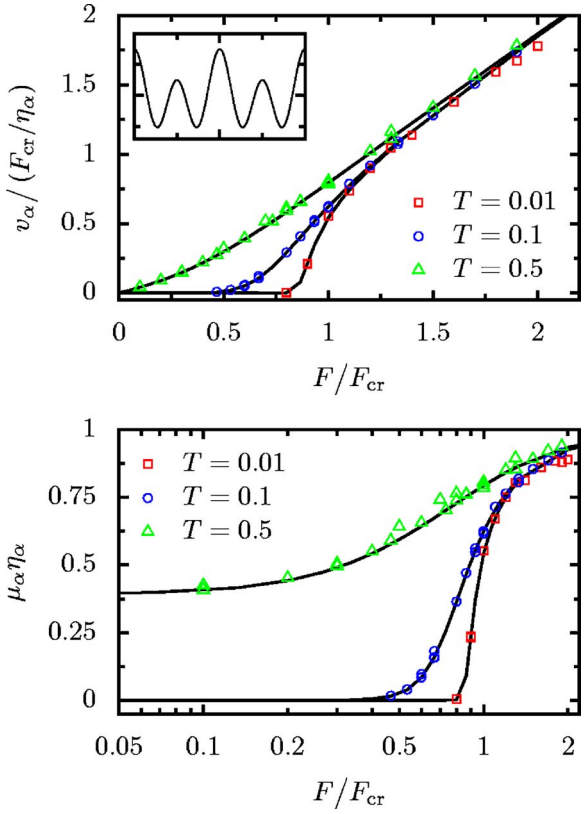

FIG. 4. (Color online) Same as in Fig. 3, for the double-hump potential, cf. Eq. (21).

and (21). In the case of the ratchetlike potential (22) also the results for negative values of the tilting force F are depicted.

We have computed the fractional current and mobility for various values of α in the interval $[0.1,1]$. Remarkably, they do not depend on the value of the fractional exponent α. For a given temperature T, all numerical values of $v_\alpha(F)/(F_{cr}/\eta_\alpha)$ and $\mu_\alpha(F)\eta_\alpha$ (depicted with symbols in Figs. 3–5) coincide with the theoretical curves resulting from Eq. (17) (solid lines).

The regime of linear response at low temperatures is numerically not accessible. In this parameter regime the corresponding escape times governing the transport become far too large [6] and particles are effectively trapped in the potential minima. At values of the tilting force F close to critical at which the minima disappear, the particles become capable of escaping from the potential wells and the current is enhanced. The higher the temperature, the smaller is the tilting required to allow the particles to escape (compare the curves corresponding to different temperatures T in Figs. 3–5). At higher values of the temperature T the linear response regime is numerically observable.

For tilting forces $F \gg F_{cr}$ or for $T \gg 1$ the dynamics approaches the behavior of a free CTRW that is exposed to a constant bias [19,25,31].

IV. PROBABILITY DENSITIES

The formal analogy between the normal and fractional diffusion which emerges from the similarity between the Fokker-Planck and fractional Fokker-Planck equations for the current with the well-known Stratonovich formula and its generalization obtained for fractional diffusion [25] masks some basic physical differences. For this reason we investigate and discuss here the time-dependent probability density in configuration space as well as the density of the current variable.

A. Time evolution

The time evolution of the space probability density $P(x,t)$ in the case of anomalous diffusion is markedly different from that of normal diffusion (see Refs. [19,31]). While for normal Brownian motion, under the influence of a constant external bias, the initial probability packet both spreads and translates on the same time scale, one observes in fractional diffusion mainly a spreading only towards the direction of the bias [19,31]. The probability density $P(x,t)$ of particles diffusing anomalously in a washboard potential assumes this latter feature and, at the same time, undergoes the same space-periodic modulation observed in normal diffusion, being typical for motion in a periodic potential. This is illustrated in Fig. 6 in which the anomalous probability density in a washboard potential for $\alpha=0.5$ (lower row) is compared with the corresponding probability density for normal diffu-

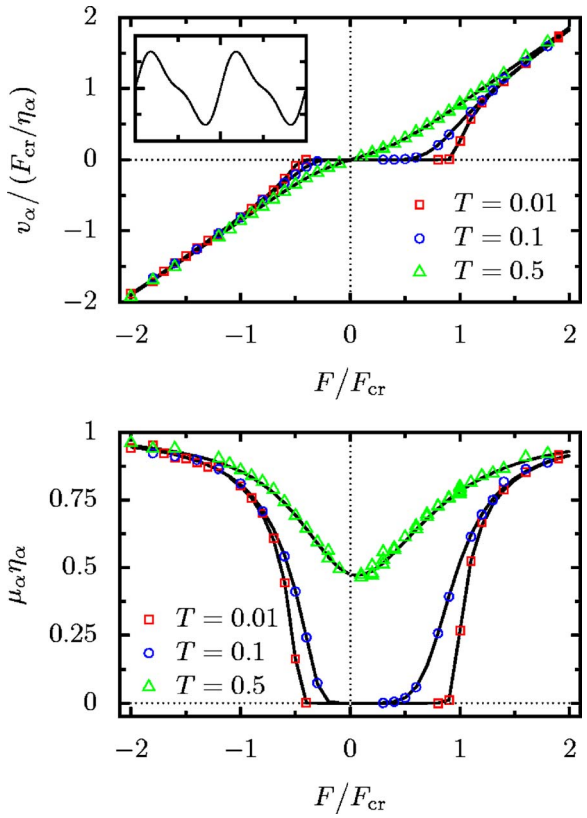

FIG. 5. (Color online). Same as in Fig. 3, for the ratchet potential, cf. Eq. (22). Here also negative tilting is studied.

sion (upper row). The data of the example in Fig. 6 have been obtained for a tilted cosine potential with $F/F_{cr}=1$ and at $T=0.1$.

B. Reduced probability density

The probability density $P(x,t)$ associated with a normal diffusion process in a washboard potential cannot relax towards a stationary, asymptotic density, due to the open-boundary nature of the system. However, the reduced asymptotic space probability density

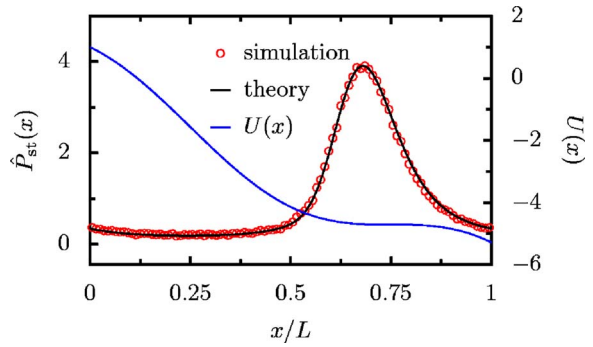

FIG. 7. (Color online). Normalized theoretical stationary, reduced probability density $\hat{P}_{st}(x)$ for $F/F_{cr}=1$, $T=0.1$, and $\alpha=0.5$, computed from Eqs. (25) and (A9) (solid line) and corresponding numerical data (circles) at time $t=5$: left y axis. Also the underlying potential $U(x)=\cos(x)-Fx$ is depicted: right y axis.

$$\hat{P}(x,t)=\sum_n P(nL+x,t), \quad n\in\mathbb{Z}, \tag{24}$$

a periodic function by definition, does relax to an asymptotic stationary density. Remarkably, in fractional diffusion, the probability density reaches the same stationary density as in the case of normal diffusion. The corresponding proof follows along the same lines of reasoning leading to the asymptotic fractional current $v_\alpha(F)$ which is formally equivalent to the Stratonovich formula valid in normal diffusion [25], as detailed also in the Appendix. This result is depicted in Fig. 7 for the case of diffusion taking place in a tilted cosine potential.

The form of the asymptotic reduced probability density $\hat{P}_{st}(x)$ is given by

$$\hat{P}_{st}(x)=\mathcal{N}^{-1}\exp[-\beta U(x)]\int_x^{x+L} dx'\exp[\beta U(x')], \tag{25}$$

where $\mathcal{N}$ is a normalization factor (see the Appendix).

Even if the stationary probability density (depicted with solid lines in Figs. 7 and 8) is the same, the relaxation to this stationary density is, however, very distinct for normal and anomalous diffusion, respectively, as shown in Fig. 8.

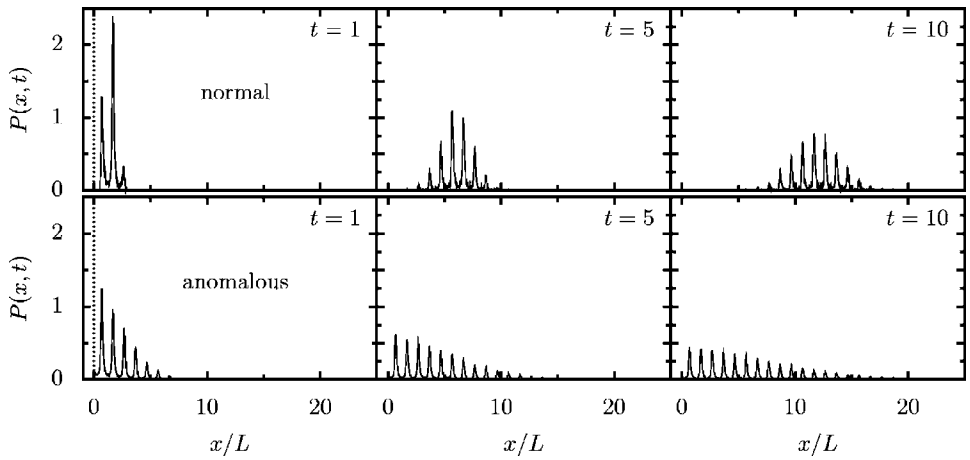

FIG. 6. Comparison between the time evolution of the probability density $P(x,t)$ in the case of normal diffusion (above) and anomalous diffusion with $\alpha=0.5$ (below) in a tilted cosine potential at various evolution times t. This setup has been calculated for the following parameter set: $T=0.1$, $F/F_{cr}=1$, and a cosine potential. Dotted lines at $t=0$ represent the initial conditions $P(x,0)=\delta(x)$; i.e., all particles start out from the same position $x=0$.

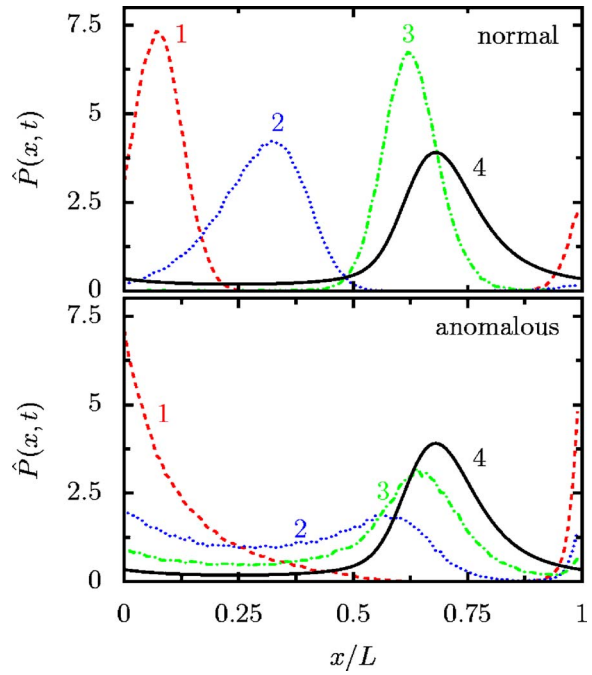

FIG. 8. (Color online) The time evolution for normal (above) and anomalous (below) diffusion of the reduced probability density $\hat{P}(x,t)$ within the first period $x \in [0,L)$ defined according to Eq. (24). In this example, the potential is $U(x)=\cos(x)-Fx$, with $F/F_{cr}=1$, the temperature is $T=0.1$, and the anomalous diffusion process corresponds to $\alpha=0.5$. The curve labels 1, 2, and 3 correspond to increasing values of time: 10^{-3}, $3\cdot10^{-3}$ and $9\cdot10^{-3}$ for the normal process, and 10^{-4} and $1.5\cdot10^{-3}$ and 10^{-2} for the anomalous case. The solid lines (labelled as 4 to indicate the time sequence) represent the theoretical stationary solution defined by Eq. (25) and practically coincide with the asymptotic numerical density.

In the case of normal diffusion, at any time instant t, the density has only one maximum, which moves from the initial position ($x=0$) toward its asymptotic position $x=x'$. At the same time it undergoes a spreading process towards the stationary density. As more particles reach the area around $x=x'$, the peak begins to grow, eventually spreading again to relax to the stationary solution $\hat{P}_{st}(x)$ (Fig. 8, upper figure).

In clear contrast, for a case with anomalous diffusion the initial probability density undergoes a spreading in the direction of the bias. While the initial maximum of the density remains at $x=0$, a second maximum emerges at $x \approx x'$, which continues to grow in weight as the density approaches the stationary shape $\hat{P}_{st}(x)$ (Fig. 8, lower figure).

C. Velocity probability density

For a particular trajectory realization $x^{(n)}(t)$, the corresponding (sub)velocity reads

$$v_\alpha^{(n)} := \Gamma(\alpha+1)[x^{(n)}(t) - x_0^{(n)}]/t^\alpha, \tag{26}$$

where $n \in 1,\ldots,N$ and $x_0^{(n)}=x^{(n)}(t_0)$. This (sub)velocity is a random variable, and one can study the corresponding probability density. One observes a spreading of the velocities corresponding to the broad spreading in space discussed above. The probability density for the velocity is depicted in Fig. 9 for a periodic substrate cosine potential, for $F/F_{cr}=1$, $T=0.1$, and $\alpha=0.5$. While the probability density for this velocity variable for normal diffusion (note the solid line, right y axis) possesses a Gaussian shape, in the anomalous case this probability density (see the dashed line, left y axis) assumes a very broad shape which falls off exponentially. Notably, however, the two densities have the same average, given by the Stratonovich formula, and indicated by the vertical dotted line in Fig. 9.

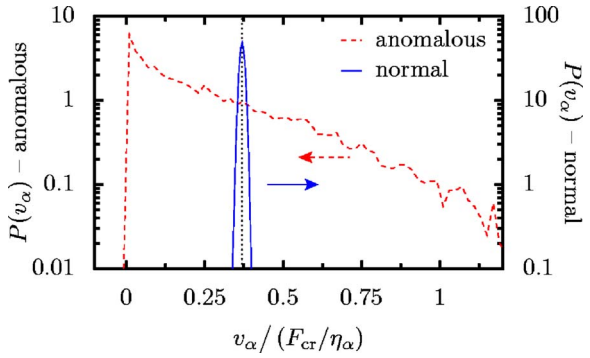

FIG. 9. (Color online) Anomalous (dashed line) and normal (solid line) probability densities of the (sub)velocity, computed according to Eq. (26) at $t=1000$ in rescaled time units. The potential, tilt, temperature, and α value are the same as in Fig. 8. The arrows point to the corresponding y axes. Despite the very different shapes, the two probability densities possess the same average value as given by the (fractional) Stratonovich formula (17), indicated with the vertical dotted line.

V. DISCUSSION AND RESUME

In the field of anomalous transport the main attention thus far has focused on the motion under the action of a constant or linear external force. With this work, we have investigated the continuous-time random walk with power-law-distributed residence times under the combined action of a space-periodic force and an external bias, thereby elucidating in more detail parts of our previous findings in Ref. [25].

The numerical algorithm for the simulation of fractional Fokker-Planck dynamics has been detailed via the underlying CTRW. The application of this algorithm deserves to be commented on in greater detail. First, the effect of the replacement of the Mittag-Leffler by the Pareto distribution does not affect the anomalous transport properties in the asymptotic limit. However, given the finite time available for doing simulations a difference can still be present if the parameter α assumes values close to 1—i.e., close to the limit of normal diffusion. Here, the use of the Mittag-Leffler distribution, which precisely matches the fractional Fokker-Planck description, is used preferably. Otherwise, one must increase the overall time of simulations to arrive at convergent results. In order to study the fractional diffusion problem on the whole time scale, the use of the Mittag-Leffler probability density is thus unavoidable.

Second, the weak ergodicity breaking [32] makes it impossible to obtain the averaged value of anomalous current

with a single time average over a single-particle trajectory. Here occurs a profound difference with the case of normal diffusion. Such a time-averaged quantity is itself randomly distributed, as shown by the broad density in Fig. 9. In clear contrast to the situation with normal diffusion, for anomalous diffusion the current probability density is very broad and with a peak at zero. Nevertheless, the average value of the current agrees very well with the theoretical Stratonovich value, as given by Eq. (17). These results in turn are close in spirit to recent work by Bel and Barkai on the weak ergodicity breaking for a spatially confined fractional diffusion [32].

The results on the averaged current and its density are complemented by the those concerning the spatial probability density of the particle ensemble as described by the fractional Fokker-Planck equation, both in the time-dependent case and for the appropriately chosen stationary regime. The strongly asymmetric character of the spreading process of the probability densities in Fig. 6 for the anomalous situation is clearly in line with the nonergodic character of the transport discussed above.

Furthermore, a new intriguing challenge concerns the universality class of the single-particle current probability densities within the CTRW underlying the fractional Fokker-Planck description. Ensemble averaging is indispensable for obtaining a mean value of the anomalous current in agreement with the theoretical results, as shown for various potential shapes. In particular the results depicted in Fig. 5 imply the emergence of rectification properties when the potential tilt is alternating in time. The anomalous diffusion ratchet problem is, however, highly nontrivial and complex because of intrinsic aging effects. For this reason, this objective is left for a future, separate study. We remark that it is presently not obvious whether an adiabatic driving limit exists at all.

We are confident that future work will help to clarify further and shed more light on all these intriguing issues and problems.

ACKNOWLEDGMENTS

We thank E. Barkai for useful discussions. This work has been supported by the ESF STOCHDYN project, the Archimedes Foundation and the Estonian Science Foundation through Grant No. 6789 (E.H.), the DFG via research center, SFB-486, project A10, and the Volkswagen Foundation, via project No. I/80424.

APPENDIX: STATIONARY (SUB)CURRENT AND PROBABILITY DENSITY IN A WASHBOARD POTENTIAL

We start from the reduced probability density and the corresponding current—i.e.,

$$\hat{P}(x,t) = \sum_n P(nL + x,t), \tag{A1}$$

$$\hat{J}(x,t) = \sum_n J(nL + x,t), \quad n \in \mathbb{Z}. \tag{A2}$$

By definition these functions obey periodic boundary conditions $\hat{P}(x+L,t)=\hat{P}(x,t)$ and $\hat{J}(x+L,t)=\hat{J}(x,t)$. If $P(x,t)$ is normalized—e.g., $\int_{-\infty}^{+\infty} dx P(x,t)=1$—then $\hat{P}(x,t)$ preserves the same normalization in any x interval (x_0,x_0+L). The condition of stationarity, obtained by letting the Caputo derivative equal to zero in the continuity equation,

$$D_*^{\alpha}\hat{P}(x,t) = -\frac{\partial \hat{J}(x,t)}{\partial x}, \tag{A3}$$

defines the reduced equilibrium probability density $\hat{P}_{\mathrm{st}}(x)$. For both normal and fractional diffusion equations, by integrating the resulting expression in x, one obtains $v_\alpha/L = \hat{J}_{\mathrm{st}}(x)$—i.e., explicitly,

$$-\frac{v_\alpha}{L} = \kappa_\alpha \exp[-\beta U(x)]\frac{d}{dx}\{\exp[\beta U(x)]\hat{P}_{\mathrm{st}}(x)\}, \tag{A4}$$

where the integration constant v_α/L is the one-dimensional flux. Multiplying both sides by $\exp[\beta U(x)]$, integrating again between x and $x+L$, and using the conditions $\hat{P}_{\mathrm{st}}(x+L) = \hat{P}_{\mathrm{st}}(x)$ and $U(x+L)=U(x)-\beta FL$,

$$-v_\alpha L^{-1}\int_x^{x+L} dx' \exp[\beta U(x')] = \kappa_\alpha \exp[\beta U(x)]\hat{P}_{\mathrm{st}}(x)[\exp(-\beta FL) - 1]. \tag{A5}$$

One can now multiply both sides by $\exp[-\beta U(x)]$ and perform the final integration between $x=0$ to $x=L$. Using the normalization of $\hat{P}_{\mathrm{st}}(x)$ in the x interval $(0,L)$,

$$-v_\alpha L^{-1}\int_0^L dx \exp[-\beta U(x)]\int_x^{x+L} dx' \exp[\beta U(x')] = \kappa_\alpha[\exp(-\beta FL) - 1]. \tag{A6}$$

From here one can obtain the explicit expression for the current,

$$v_\alpha = \frac{\kappa_\alpha L[1 - \exp(-\beta FL)]}{\int_0^L dx \exp[-\beta U(x)]\int_x^{x+L} dx' \exp[\beta U(x')]}. \tag{A7}$$

The stationary reduced probability density can be obtained by inverting Eq. (A5),

$$\hat{P}_{\mathrm{st}}(x) = \mathcal{N}^{-1}\exp[-\beta U(x)]\int_x^{x+L} dx' \exp[\beta U(x')], \tag{A8}$$

where the normalization constant is given by

$$\mathcal{N} = \kappa_\alpha L[1 - \exp(-\beta FL)]/v_\alpha. \tag{A9}$$

[1] P. Hänggi and F. Marchesoni, Chaos **15**, 026101 (2005).
[2] P. Hänggi, A. Alvarez-Chillida, and M. Morillo, Physica A **351**, XI (2005) (special issue).
[3] P. Hänggi and F. Marchesoni, Physica A **325**, XV (2003) (special issue).
[4] J. A. Freund and T. Pöschel,Lect. Notes Phys. **557**, 1 (2000).
[5] W. Ebeling and I. M. Sokolov, *Statistical Thermodynamics and Stochastic Theory of Nonequilibrium Systems*, Ser. Adv. Stat. Mech. 8 (World Scientific, Singapore, 2005).
[6] P. Hänggi, P. Talkner, and M. Borkovec, Rev. Mod. Phys. **62**, 251 (1990).
[7] M. Borromeo and F. Marchesoni, Chaos **15**, 026110 (2005).
[8] R. D. Astumian and P. Hänggi, Phys. Today **55**(11), 33 (2002).
[9] P. Reimann and P. Hänggi, Appl. Phys. A: Mater. Sci. Process. **75**, 169 (2002).
[10] P. Hänggi, F. Marchesoni, and F. Nori, Appl. Phys. (Leipzig) **14**, 51 (2005).
[11] F. Jülicher, A. Ajdari, and J. Prost, Rev. Mod. Phys. **69**, 1269 (1997).
[12] Y. Kafri, D. K. Lubensky, and D. R. Nelson, Biophys. J. **86**, 3373 (2004).
[13] J. W. Haus and K. W. Kehr, Phys. Rep. **150**, 263 (1987).
[14] J. P. Bouchaud, A. Comtet, A. Georges, and P. Le Doussal, Ann. Phys. (N.Y.) **201**, 285 (1990).
[15] J. P. Bouchaud and A. Georges, Phys. Rep. **195**, 127 (1990).
[16] B. Derrida, J. Stat. Phys. **31**, 433 (1983).
[17] I. M. Sokolov and J. Klafter, Chaos **15**, 026103 (2005).
[18] R. Metzler and J. Klafter, Phys. Rep. **339**, 1 (2000).
[19] H. Scher and E. W. Montroll, Phys. Rev. B **12**, 2455 (1975).
[20] B. Lindner and L. Schimansky-Geier, Phys. Rev. Lett. **89**, 230602 (2002).
[21] R. Metzler, E. Barkai, and J. Klafter, Phys. Rev. Lett. **82**, 3563 (1999).
[22] E. Barkai, Phys. Rev. E **63**, 046118 (2001).
[23] I. M. Sokolov, J. Klafter, and A. Blumen, Phys. Today **55**(11), 48 (2002).
[24] R. Gorenflo and F. Mainardi, in *Fractals and Fractional Calculus in Continuum Mechanics*, edited by A. Carpinteri and F. Mainardi (Springer, Wien, 1997), p. 223.
[25] I. Goychuk, E. Heinsalu, M. Patriarca, G. Schmid, and P. Hänggi, Phys. Rev. E **73**, 020101(R) (2006).
[26] Under this condition one can also safely replace $\beta(U_{i\pm1/2}-U_i)$ with $\beta(U_{i\pm1}-U_i)/2$ without a violation of the detailed balance condition, as done for the discretization procedure used in Ref. [25].
[27] G. H. Weiss, *Aspects and Applications of the Random Walk* (North-Holland, Amsterdam, 1994).
[28] F. Mainardi, A. Vivoli, and R. Gorenflo, Fluct. Noise Lett. **5**, L291 (2005).
[29] W. H. Press, B. P. Flannery, S. A. Teukolsky, and W. T. Vetterling, *Numerical Recipes in C: The Art of Scientific Computing*, 2nd ed. (Cambridge University Press, Cambridge, England, 1992).
[30] R. L. Stratonovich, Radiotekh. Elektron. (Moscow) **3**(4), 497 (1958); V. I. Tikhonov, Avtom. Telemekh. **20**(9), 1188 (1959); R. L. Stratonovich, *Topics in the Theory of Random Noise* (Gordon and Breach, New York, 1967), Vol. II; Yu. M. Ivanchenko and L. A. Zil'berman, Zh. Eksp. Teor. Fiz. **55**, 2395 (1968) [Sov. Phys. JETP **28**, 1272 (1969)]; V. Ambegaokar and B. I. Halperin, Phys. Rev. Lett. **22**, 1364 (1969).
[31] M. Shlesinger, J. Stat. Phys. **10**, 421 (1974).
[32] G. Bel and E. Barkai, Phys. Rev. Lett. **94**, 240602 (2005).